Development of 3-D Anatomically-Detailed Mathematical Models of the Sinoatrial and Atrioventricular Nodes

J Li[1], H Dobrzynski[1], ID Greener[1], VP Nikolski[2], M Yamamoto[1], R Billeter[1], IR Efimov[2], MR Boyett[1]

[1]University of Leeds, Leeds, UK
[2]Washington University, St. Louis, USA

Abstract

We used multiple techniques to construct 3D anatomical models of the rabbit sinoatrial node (SAN) and atrioventricular node (AVN). The 3D SAN model includes atrial muscle (only atrial cells), central SAN (only central SAN cells), peripheral SAN (a mixture of peripheral SAN cells, 'central' SAN cells and atrial cells), connective tissue and the sinus node artery. The 3D AVN model includes atrial muscle, ventricular muscle, AVN, a possible transitional zone (loosely packed atrial cells) and connective tissue (including the tendon of Todaro).

1. Introduction

The cardiac conduction system includes three important parts: the sinoatrial node (SAN), the atrioventricular node (AVN) and the His-Purkinje system. Figure 1 shows the location of the SAN and AVN. The SAN is the 'natural pacemaker' of the heart and it controls the heart rate. The AVN is the 'electrical bridge' between the atria and ventricles. The AVN is responsible for the conduction delay present during the cardiac cycle.

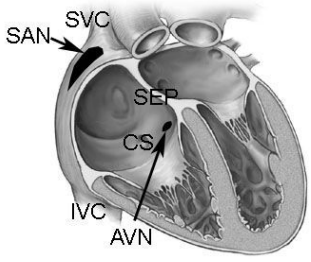

Figure 1. This figure of the heart shows the location of the SAN and AVN. CS: coronary sinus; IVC: inferior vena cava; SEP: interatrial septum; SVC: superior vena cava.

The SAN and AVN are complex and heterogeneous in terms of function and morphology. To accurately simulate the generation and conduction of cardiac electrical activity requires detailed anatomical and electrophysiological models. The purpose of this study was to construct three dimensional (3D) anatomical models of the SAN and AVN. The models can be used in combination with electrophysiological models to investigate how electrical activity is generated and conducted.

2. Methods

Intact SAN and AVN preparations were dissected from rabbit hearts. Preparations were fixed in 10% neutral buffered formalin for 24 h, washed in 70% ethanol for 2 h and embedded in paraffin.

To construct 3D models, ~60 serial groups of three sections were cut throughout the SAN and AVN preparations. In each group, one section was stained with Masson's trichrome for histology and the others were stained by immunoenzyme for middle neurofilament (NF) and connexin43 (Cx43). Masson's trichrome stained sections provided the outline of the tissue and the distribution of myocytes and connective tissue. NF and Cx43 immunolabelled sections were used to divide the myocytes into working myocardium and nodal cells.

The construction of the SAN model will be described; the construction of the AVN model was analogous. MATLAB (version 6.5; The MathWorks, Inc., Matick, MA, USA) was used to analyse the images and construct the 3D model. **Step 1.** To determine the outline of the Masson's trichrome stained section (Figure 2A), image processing functions were used. The complement of the image was obtained, so that pixel values of structures were higher than those of the background. Then, the resulting image was converted to a binary image based on the global image threshold, which was computed using Otsu's method. We extracted large objects from this thresholded image using morphologic closing and opening operations in succession (Figure 2B). Finally, the resulting image was modified using custom-written code to add lines, fill holes, and erase artifacts (Figure 2C). **Step 2.** Next the outline of the myocytes in the Masson's trichrome stained section was determined. Abode Photoshop (version 7.0) was used to highlight the myocytes (Figure 2D) and then the methods described above were used to determine the outline of the myocytes (Figure 2E and F). Finally, the tissue and myocyte profiles were combined to obtain a model section (Figure

2G). This showed the distribution of myocytes and connective tissue (fibroblasts, adipocytes and collagen fibres). **Step 3.** The Masson's trichrome stained section was compared with the NF and Cx43 labelled sections to distinguish three zones of myocytes: atrial (NF-negative, Cx43-positive), peripheral SAN (a mixture of cell types) and central SAN (NF-positive, Cx43-negative) as shown in Figure 3. Because the three adjacent sections were not identical, these three zones had to be tracked manually. The Masson's trichrome stained sections were also used to determine the position of the sinoatrial ring bundles and sinus node artery. This information was incorporated into the model sections.

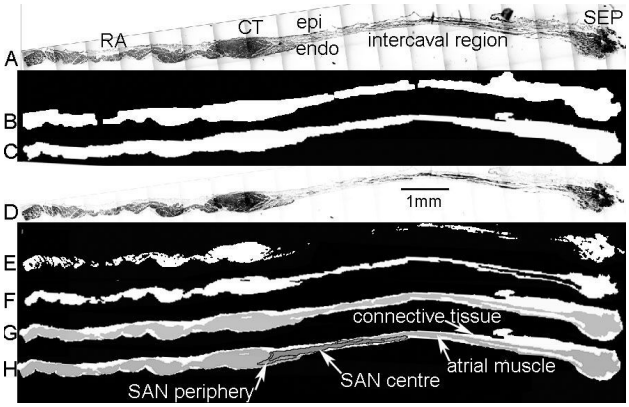

Figure 2. A is a SAN section stained with Masson's trichrome. CT: crista terminalis; endo: endocardium; epi: epicardium; RA: right atrial free wall. B shows the binary image after applying image processing functions. C shows the image after manual modification. D is a SAN image in which myocytes were highlighted. E shows the binary image of the myocytes after applying image processing functions. F shows the image of the myocytes after manual modification. G shows the model section in which the myocytes and outline of the tissue have been combined. H shows the final model section, which includes four regions: connective tissue, atrial muscle (only atrial cells), SAN periphery (mixture of peripheral SAN cells, 'central' SAN cells and atrial cells) and SAN centre.

Step 4. Sections could be misaligned and distorted and they had to be aligned. A misaligned image was rotated using linear conformal transformation. A distorted image was corrected using polynomial transformation. **Step 5.** The cubic smoothing spline was used to smooth the lines of the model sections. **Step 6.** Linear interpolation was used to interpolate model sections between every original pair of model sections (thus doubling the number of model sections). After interpolation, the new model sections had to be corrected manually. **Step 7.** The 3D array model was obtained by stacking the two-dimensional model sections. To visualize the array model, the 3D array was smoothed and the isosurface was computed. **Step 8.** The centre and diameter of the sinus node artery in each model section was determined and then the sinus node artery was constructed.

3. Results

3.1. 3D sinoatrial node model

In the SAN, three myocardial cell types were identified: central SAN cells (NF-positive/Cx43-negative), peripheral SAN cells (NF-positive/Cx43-positive) and atrial cells (NF-negative/Cx43-positive). Compared with the central SAN cells, the quantity of peripheral SAN cells was less and the organization was more irregular. Figure 3 shows that the distribution of the different cell types was complex and heterogeneous.

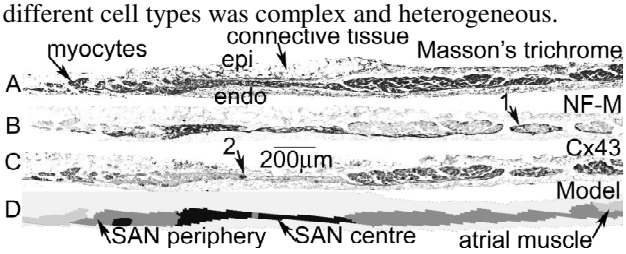

Figure 3. A shows a SAN section stained with Masson's trichrome. B and C show adjacent SAN sections labelled for NF and Cx43. D shows the resulting model section. Atrial muscle: only atrial cells with connective tissue. SAN periphery: mixture of peripheral SAN node cells, 'central' SAN cells and atrial cells with connective tissue. SAN centre: only central SAN cells with connective tissue.

In Figure 3D, the SAN centre consists only of central SAN cells with connective tissue. The atrial muscle consists only of atrial cells with connective tissue. The SAN periphery consists of a mixture of cells (peripheral SAN cells, 'central' SAN cells and atrial cells) with connective tissue.

Figure 4 shows the 3D SAN model without the outer connective tissue layer. Figure 4A shows that the SAN centre was located within the intercaval region between the superior and inferior vena cava. The SAN periphery is the only connection between the SAN centre and atrial muscle. Hence, the SAN periphery is the only conduction pathway from the SAN centre to the atrial muscle. The majority of the SAN periphery lies on the endocardial surface of the atrial muscle. From Figure 4A, it can be seen that there are 'holes' (for example highlighted by arrows). In the 'holes' there are few or no myocytes and only connective tissue. There is a lack of myocytes between the SAN centre and the interatrial septum (Figure 4A, arrow 1) and this corresponds to a conduction

block zone [1]. There is also a lack of myocytes between the crista terminalis and the intercaval region (Figure 4A, arrow 2). Figure 4B shows just the SAN periphery and centre with the left and right sinoatrial ring bundles (a landmark) - the atrial muscle has been removed and this reveals the sinus node artery. It can be seen that the sinus node artery is located just beside the SAN centre. Figure 4C and D shows top down views of the SAN model. Figure 4C shows all myocytes (connective tissue has been removed). Figure 4D shows only the SAN cells. Figure 4D shows that the SAN periphery connects with the crista terminalis from both the epicardial and endocardial sides, like a 'hand'.

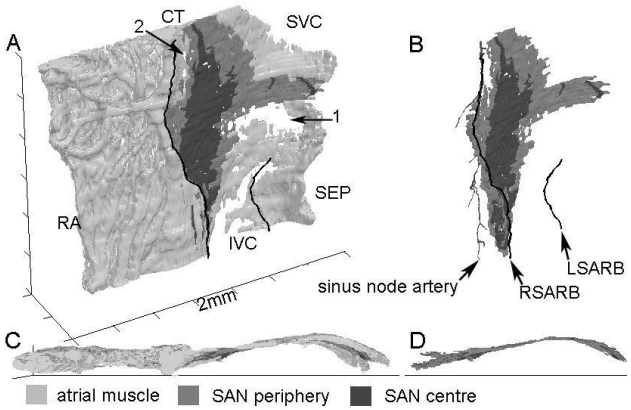

Figure 4. A shows the 3D SAN model without outer connective tissue layer. Arrows 1 and 2 show regions with few or no myocytes. B shows the SAN centre and periphery with the sinus node artery. C shows a top down view of the 3D SAN model without the outer connective tissue layer. D shows a top down view of the SAN centre and periphery. LSARB: left sinoatrial ring bundle; RSARB: right sinoatrial ring bundle.

3.2. 3D atrioventricular node model

In the AVN preparation, three myocardial cell types were identified: atrial and ventricular cells (NF-negative/Cx43-positive) and AVN cells (NF-positive/primarily Cx43-negative).

Figure 5 shows the 3D AVN model without the outer connective tissue layer. The model includes atrial muscle, ventricular muscle, loosely packed atrial muscle (transitional zone?), AVN and the tendon of Todaro (a landmark). From Figure 5A, it can be seen that the AVN is located between the atrial and ventricular muscle. The AVN tissue is located close to the ventricular muscle at the His bundle end, but the AVN tissue of the compact node and posterior nodal extension is located close to the atrial muscle. There is abundant connective tissue within or surrounding the AVN tissue. There is a region of loosely packed atrial muscle between the AVN and the rest of the atrial muscle (compact) (Figure 5A and B). This region could be a transitional zone and it could be the fast pathway into the AVN [2]. The loosely packed atrial muscle lies over the open part of the AVN near the compact node.

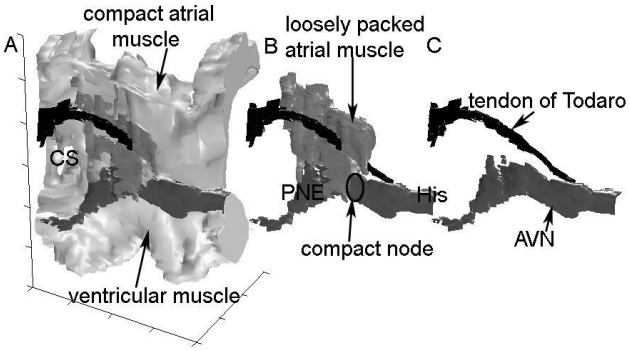

Figure 5. A shows the 3D AVN model without the outer connective tissue layer. B shows the AVN with the loosely packed atrial muscle (transitional zone?) and the tendon of Todaro (a landmark). C shows the AVN and tendon of Todaro. His: His bundle; PNE: posterior nodal extension

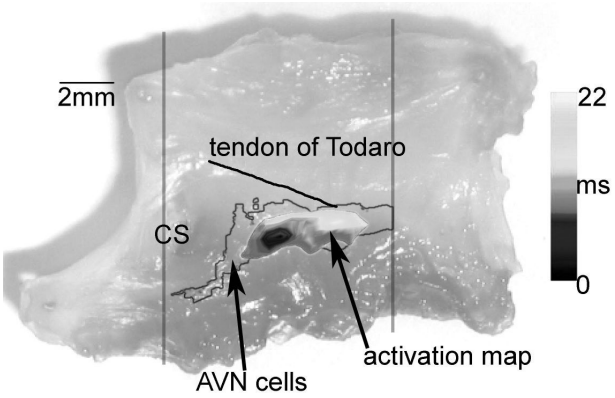

Figure 6. The figure shows the activation map during AVN pacemaking and an outline of the AVN tissue superimposed on the AVN preparation

Figure 6 shows the activation map during AVN pacemaking and an outline of the AVN tissue superimposed on the AVN preparation. The leading pacemaker site during AVN pacemaking corresponds to the posterior nodal extension. We found that the cell arrangement at the SAN leading pacemaking site and the AVN leading pacemaking site is similar: interweaving nodal cells with abundant connective tissue.

4. Discussion and limitations

The 3D SAN and AVN models, which we have developed, are anatomically-detailed 3D models. The models can be used to simulate how electrical activity is

generated and conducted. However, the models do not include all known complexities. These complexities in the case of the SAN are described below.

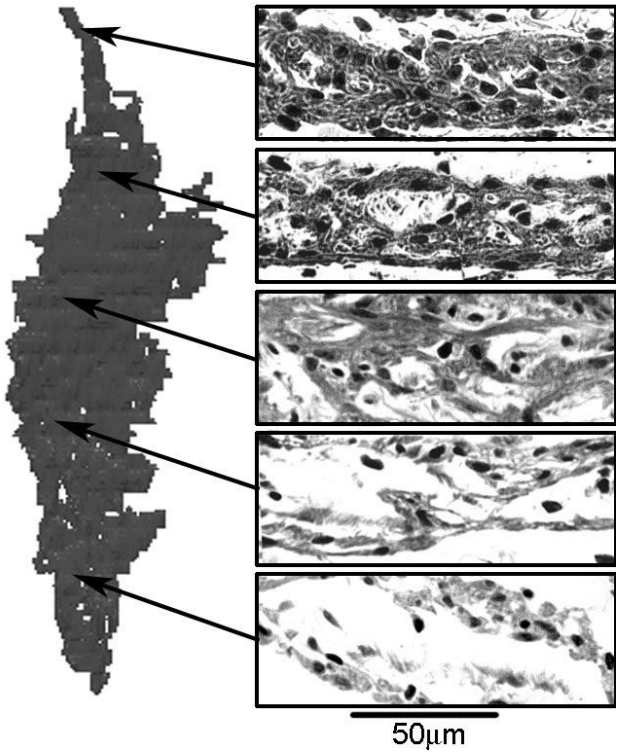

Figure 7. The left panel shows the SAN centre from the 3D model. The right panels show Masson's trichrome stained sections from the positions shown.

The 3D SAN model includes three major regions: atrial muscle, SAN periphery and SAN centre. The most complex region is the SAN periphery. The SAN periphery is the only pathway from the SAN centre to the atrial muscle and, hence, it is important to understand how the SAN cells connect with the atrial muscle within the SAN periphery. We found that there were four types of connection between the SAN cells and the atrial muscle. One is a root-like connection (data not shown): strings of SAN cells run into the atrial muscle like a root. Another is a socket-like connection: a group of SAN cells form a socket (or half socket) and hold an atrial muscle bundle (Figure 3B, arrow 1). A third one is a sandwich-like connection: a SAN cell layer connects with an atrial muscle layer in a sandwich-like manner (data not shown). Finally, there is irregular connection, particularly at the foot of the crista terminalis.

It was found that there is an atrial muscle bundle running parallel with the crista terminalis and it is inserted into the SAN centre (Figure 3C, arrow 2). It may be one of the reasons that within the SAN the conduction velocity parallel to the crista terminalis is faster than the conduction velocity perpendicular to the crista terminalis.

There is abundant connective tissue within the SAN centre compared with the atrial muscle. Abundant connective tissue is also found at the foot of the crista terminalis. The reason may be to protect the SAN centre from the influence of the more hyperpolarized crista terminalis - atrial muscle.

The size of the SAN cells is smaller than that of the atrial cells. The cell density is different throughout the SAN preparation. The cell density within the atrial muscle is higher than the cell density within the SAN. Within the SAN centre, the cell density is reduced from the top (near the SVC) towards the bottom (near the IVC) as shown in Figure 7.

It is important to know cell orientation for electrophysiological modelling. The atrial cells run along the atrial muscle bundles within the right atrial free wall. Cell orientation is very complicated throughout the intercaval region. Within the SAN centre, the cells can be interweaving (Figure 7).

Acknowledgements

We would like to thank Sally E. Wright for help with the SAN preparation, and Tim Lee for help with the AVN preparation. The anti-NF165 antibody was obtained from Dr. Simon H. Parson.

References

[1] Boyett MR, Honjo H, Kodama I. The sinoatrial node, a heterogeneous pacemaker structure. Cardiovasc Res. 2000; 47: 658-687.

[2] Mazgalev TN, Ho SY, Anderson RH. Anatomic-elactrophysiological correlations concerning the pathways for atrioventricular conduction. Circulation. 2001; 103: 2660-2667.

Address for correspondence

Mark Boyett
School of Biomedical Sciences
University of Leeds
Leeds, LS2 9JT
UK
m.r.boyett@leeds.ac.uk